Superlattices and Microstructures 127 (2019) 157–164

Contents lists available at ScienceDirect

Superlattices and Microstructures

journal homepage: www.elsevier.com/locate/superlattices

Controlling the optical absorption properties of δ-FETs by means of contact voltage and hydrostatic pressure effects

O. Oubram [a, *], O. Navarro [b], I. Rodriguez-Vargas [c], L.M. Gaggero-Sager [d], H.G. Noverola [e, f]

[a] Facultad de Ciencias Químicas e Ingeniería, Universidad Autónoma del Estado de Morelos, Av. Universidad 1001 Col. Chamilpa, Cuernavaca, 62209, Mexico
[b] Unidad Morelia del Instituto de Investigaciones en Materiales, Universidad Nacional Autónoma de México, Antigua Carretera a Pátzcuaro No. 8701 Col. Ex-Hacienda de San José de la Huerta, Morelia, 58190, Mexico
[c] Unidad Académica de Física, Universidad Autónoma de Zacatecas, Calzada Solidaridad Esquina con Paseo la Bufa S/N, 98060, Zacatecas, Mexico
[d] CIICAP-(IICBA), Universidad Autónoma del Estado de Morelos, Av. Universidad 1001 Col. Chamilpa, Cuernavaca, 62209, Mexico
[e] IICBA. Universidad Autónoma del Estado de Morelos, Av. Universidad 1001 Col. Chamilpa, Cuernavaca, 62209, Mexico
[f] División Académica de Ingeniería y Arquitectura, Universidad Juárez Autónoma de Tabasco, Carretera Cunduacán-Jalpa de Méndez Km.1 Col. La Esmeralda, Cunduacán, Tabasco, 86690, Mexico

ARTICLE INFO

Article history:
Available online 5 December 2017

Keywords:
Absorption coefficient
δ-FET
Hydrostatic pressure effects
Contact voltage effects

ABSTRACT

The effects of contact voltage and hydrostatic pressure on subband structure and optical transitions in GaAs delta-Field Effect Transistor (δ-FET) are theoretically studied. The electronic structure of δ-FET under hydrostatic pressure is determined by solving the Schrödinger equation using a theoretical model at low pressure. It is found that the subband energies and intersubband optical absorption on δ-FET are quite sensitive to the contact voltage and applied hydrostatic pressure. Wherein, a blue-shifting as hydrostatic pressure increases and a red-shifting as the contact potential increases, are shown. Our results could be important for infrared optical device applications and useful in the design of devices based on contact voltage and hydrostatic pressure-dependent optical processes.

1. Introduction

Nowadays, the communication and information technology has changed the humanity lifestyle. This change is mainly due to the built up of knowledge and transistor's technology. During all microelectronics history, transport is one of the most explored physical properties in transistors. Recently, theoretical and experimental researchers have been interested in the optical properties due to their wide application in optoelectronics [1–6]. In particular, Muravjov et al. [6] have investigated experimentally the temperature dependence of plasmonic terahertz absorption in grating-gate gallium-nitride transistor structures. Saidi et al. [1] examined theoretically the refractive index changes and absorption coefficient in AlGaN/GaN heterostructure field-effect transistors [3]. Hofstetter et al. [7] have studied the midinfrared intersubband absorption in high-electron-mobility transistors. All these results reveal that the optical properties are very sensitive to the doping concentration, the incident beam intensity and the strength of the electric field.

* Corresponding author.
E-mail address: oubram@uaem.mx (O. Oubram).

https://doi.org/10.1016/j.spmi.2017.11.062
0749-6036/

Moreover, the technological breakthrough in low-dimensional systems such as quantum dots, quantum wells and quantum wire allows to find fascinating transport and optical properties [4,5,8–14]. One of the most promising systems of these nanostructures, for optical applications, is the delta-doped quantum well DDQW [4,5,14,15]. Specifically, the coupling of two different low-dimensional systems, the delta-doped well and the field effect transistor give place to δ-FET transistor [16,17]. This coupling allows to take advantage of its optical characteristics. In fact, several studies of the optical properties in transistor type δ-FET have been reported recently [4,5].

The study of optical properties in low dimensional systems under external effects gives valuable information of how the optoelectronic properties of these systems can be modulated effectively [18–21]. However, in the case of hydrostatic pressure the optical properties of δ-FET have not been well understood so far. Raigoza et al. [10] have calculated optical absorption spectra in symmetrical doped quantum well structures in the presence of applied pressure. They observed a blue shift in the optical transitions upon increasing pressure. The pressure effect on intersubband optical absorption in a V-groove quantum wire was studied by Khordad et al. [22]. They deduced that the absorption coefficient increases towards high energies as the pressure increases. Karabulut et al. [20] investigated the dependence of optical absorption in asymmetric double quantum wells under hydrostatic pressure. The effects of hydrostatic pressure on the optical absorption coefficient in QDs have been computed by Galindez et al. [23] and Shijun Liang et al. [11]. Martínez-Orozco et al. [4] discussed nonlinear optical rectification and second and third harmonic generation in GaAs δ-FET systems under hydrostatic pressure. They have investigated the linear and nonlinear optical absorption coefficients in δ-FET under hydrostatic pressure [5], finding that intermediate pressure leads to an enhancement of both linear and nonlinear absorption, whereas for higher pressures their amplitudes are significantly quenched.

To our knowledge, this work is the first study on combined effects of contact voltage and hydrostatic pressure on the linear and nonlinear intersubband optical absorption in δ-FET. Besides, in this study was used a new theoretical model at low pressure, which is applied in δ-FET transistor. Our outcomes reveal that there is an important influence of the contact voltage and applied hydrostatic pressure on the linear and nonlinear intersubband optical absorption in *n*-type δ-FET. Moreover, the electronic structure and absorption properties of δ-FET has been studied by applying a simple theoretical model at low pressure. Our outcomes reveal that there is an important influence of the contact voltage and applied hydrostatic pressure on the linear and nonlinear intersubband optical absorption in *n*-type δ-FET.

2. Methodology

The calculation of the absorption coefficient is performed by solving the Schrödinger equation associated to the system using the effective mass approximation, obtaining the values of the wave functions and eigenvalues, effective mass and potential are functions of pressure [14,24–26].

After the energies and their corresponding wave functions is obtained, the linear absorption coefficient $\alpha^{(1)}(\omega)$ and the nonlinear absorption coefficient $\alpha^{(3)}(\omega)$ for the intersubband transitions between two subbands can be readily calculated as [27]:

$$\alpha^{(1)}(\omega) = \frac{\omega\mu c}{n_r}\left|M_{fi}\right|^2 \frac{m^* k_B T}{L_{eff}\pi\hbar^2} \times In\left\{\frac{1+\boldsymbol{exp}[(E_F-E_i)/k_BT]}{1+\boldsymbol{exp}\left[\left(E_F-E_f\right)\Big/k_BT\right]}\right\} \times \frac{\hbar/\tau_{in}}{\left(E_F-E_i-\hbar\omega\right)^2+\left(\hbar/\tau_{in}\right)^2}, \tag{1}$$

and

$$\alpha^{(3)}(\omega,I) = \frac{-\omega\mu c}{n_r}\left(\frac{I}{2\varepsilon_0 n_r}\right)\left|M_{fi}\right|^2 \frac{m^* k_B T}{L_{eff}\pi\hbar^2} \times In\left\{\frac{1+\boldsymbol{exp}[(E_F-E_i)/k_BT]}{1+\boldsymbol{exp}\left[\left(E_F-E_f\right)\Big/k_BT\right]}\right\} \times \frac{\hbar/\tau_{in}}{\left\{\left(E_F-E_i-\hbar\omega\right)^2+\left(\hbar/\tau_{in}\right)^2\right\}^2} \times \left[4\left|M_{fi}\right|^2 - \Xi\right], \tag{2}$$

where

$$\Xi = \frac{\left[\left(E_F-E_i-\hbar\omega\right)^2-\left(\frac{\hbar}{\tau_{in}}\right)^2+2\left(E_f-E_i-\hbar\omega\right)\left(E_f-E_i-\hbar\omega\right)\right]}{\left|M_{ff}-M_{ii}\right|^{-2}\left[\left(f-E_i\right)^2+\left(\frac{\hbar}{\tau_{in}}\right)^2\right]},$$

Here E_i and E_f denote the quantized energy levels for the initial and final states, respectively, L_{eff} is the effective spatial extent of electrons in subbands, I is the optical intensity of incident wave, μ is the permeability, n_r is the refractive index, c is the speed of light in free space, τ_{in} is the intersubband relaxation time (τ_{in} is a constant with numerical value of 0.14 *ps* [27]) and the dipole matrix element is defined by

$$M_{fi} = \int_{-L_0/2}^{L_0/2} \psi_f^*(z) z \psi_i(z) dz. \tag{3}$$

We introduce the relative linear absorption coefficient $\alpha_{rel}^{(1)}(\omega, P)$ [14] and relative nonlinear absorption coefficient $\alpha_{rel}^{(3)}(\omega, I, P)$:

$$\alpha_{rel}^{(1)}(\omega, P) = \frac{\alpha^{(1)}(\omega, P)}{\alpha_{10}^{(1)}(\Omega, P = 0)}, \tag{4}$$

$$\alpha_{rel}^{(3)}(\omega, I, P) = \frac{\alpha^{(3)}(\omega, I, P)}{\alpha_{10}^{(1)}(\Omega, P = 0)}, \tag{5}$$

where $\alpha_{10}^{(1)}(\Omega, P = 0)$ is the linear absorption coefficient for the intersubband transitions between the ground state and the first excited state at $P = 0$ kbar, and $\Omega = \boldsymbol{arg}[\boldsymbol{max}(\alpha_{1-0}^{(1)}(\omega, P = 0))]$ presents the value of resonance for intersubband transition 1-0.

Now, we write expressions (4) and (5) in relative effective atomic units at $T = 0$ K,

$$\alpha_{rel}^{(1)}(\omega, P) = \frac{\omega}{\Omega} \times \left|\frac{M_{fi}(0)}{M_{10}(0)}\right|^2 \times \frac{m^*(P)}{m^*(0)} \times \frac{\varepsilon(0)}{\varepsilon(P)} \times \frac{\Delta E_{fi}(0)}{\Delta E_{10}(0)} \times \frac{(\Delta E_{10}(0) - \hbar\Omega)^2 + (\hbar/\tau_{in})^2}{\left(\Delta E_{fi}(0) \frac{m^*(P)}{m^*(0)} \frac{\varepsilon(0)^2}{\varepsilon(P)^2} - \hbar\omega\right)^2 + (\hbar/\tau_{in})^2}, \tag{6}$$

$$\alpha_{rel}^{(3)}(\omega, I, P) = -\alpha_{rel}^{(1)}(\omega, P) \times \frac{\left(\frac{I}{2\varepsilon_0 n_r c}\right)\left(\frac{a_0^*(P)}{a_0^*(0)}\right)^2 \left[4\left|M_{fi}(0)\right|^2 - \mathrm{Y}\right]}{\left(\Delta E_{fi}(P) - \hbar\omega\right)^2 + (\hbar/\tau_{in})^2}, \tag{7}$$

where

$$\mathrm{Y} = \frac{\left[\left(\Delta E_{fi}(P) - \hbar\omega\right)\left(2\Delta E_{fi}(P)^2 + 1\right) - \left(\frac{\hbar}{\tau_{in}}\right)^2\right]}{\left|M_{ff}(0) - M_{ii}(0)\right|^{-2}\left[\Delta E_{fi}(P)^2 - \left(\frac{\hbar}{\tau_{in}}\right)^2\right]},$$

where $[a_0^*(P)/a_0^*(0)] = [\varepsilon(P)/\varepsilon(0)] \times [m^*(0)/m^*(P)]$ and $\Delta E_{fi}(P) = \Delta E_{fi}(0) \times [m^*(P)/m^*(0)][\varepsilon^2(0)/\varepsilon^2(P)]$, furthermore $\Delta E_{fi}(0) = E_f(0) - E_i(0)$ denotes quantized energy between the final and initial states at $P = 0$ kbar.

We define the relative matrix element as:

$$M_{fi_{rel}} = \frac{M_{fi}(P)}{M_{10}(0)}. \tag{8}$$

Writing this expression in effective atomic units, we obtain the reduced expression,

$$M_{fi_{rel}} = \frac{M_{fi}(0)}{M_{10}(0)} \times \frac{m^*(0)}{m^*(P)} \times \frac{\varepsilon(P)}{\varepsilon(0)}. \tag{9}$$

Using Eqs. (1), (2), (6) and (7) one can express the total absorption coefficient $\alpha_{rel}^{(total)}(\omega, I, P)$ as:

$$\alpha_{rel}^{(total)}(\omega, I, P) = \alpha_{rel}^{(1)}(\omega, P) + \alpha_{rel}^{(3)}(\omega, I, P). \tag{10}$$

3. Results and discussion

We now apply the above formulation to calculate the electronic structure and the optical properties. Fig. 1(a) shows the confinement potential, the wavefunctions and the subband energies for two different pressure values for a contact potential $V_c = 650$ meV and doping concentration $N_{2d} = 7.5 \times 10^{12}\mathrm{cm}^{-2}$. Solid (dashed) curves correspond to $P = 0$ ($P = 5$ kbar). As seen in this figure, the eigenfunctions and the potential are more confined, with the increase of the hydrostatic pressure.

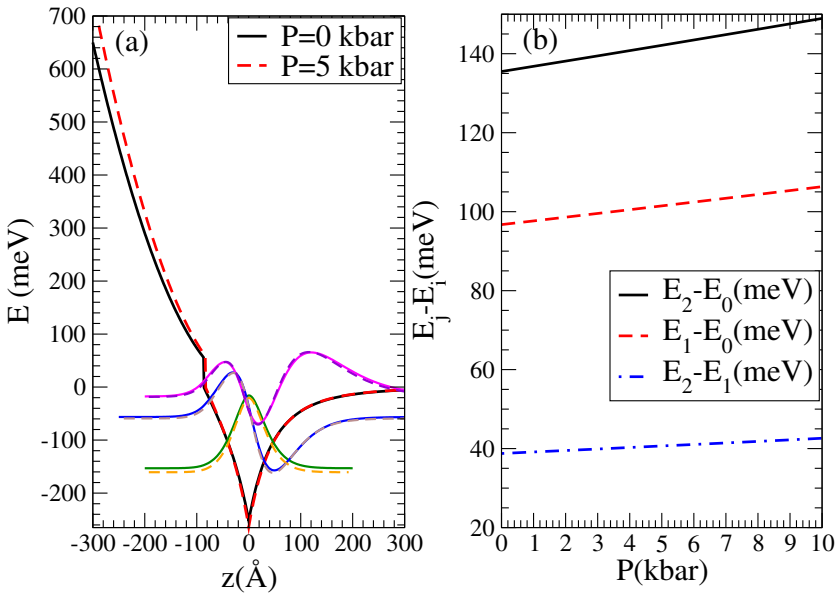

Fig. 1. (a) Confining potential profile, subband energies and their wave functions for $P = 0$ kbar (solid curves) and $P = 5$ kbar (dashed curves). The contact voltage and impurity density considered are $V_c = 650$ meV and $N_{2d} = 7.5 \times 10^{12}\text{cm}^{-2}$, respectively. (b) Energy difference between different states as a function of hydrostatic pressure with are $V_c = 650$ meV and $N_{2d} = 7.5 \times 10^{12}\text{cm}^{-2}$.

Moreover, the height of Schottky barrier is larger when $P = 5$ kbar (dashed curve) than when $P = 0$ kbar (solid curve). Savaş et al. and Oubram et al. [28,29] report this kind of behavior in metal-semiconductor structures under pressure. Additionally, the conduction band potential of δ-FET has an asymmetric configuration, which allows a nonlinear optical response. In fact, it is possible to tailor the asymmetry of the system by applying different contact potentials. The functions are more confined by the effect of the pressure, in this case the dielectric constant decreases and the effective mass increases.

Fig. 1(b) exhibits the variation of the confining energy difference as a function of the hydrostatic pressure. As seen from this figure, when the pressure increases, the energy difference $E_j - E_i$ increases. In V-groove quantum wire and delta-doped QWs [14,22] were been observed similar behavior.

The relative linear absorption coefficients as a function of photon energy for three different pressures show in Fig. 2, with $V_c = 650$ meV and $N_{2d} = 7.5 \times 10^{12}\text{cm}^{-2}$. It is noted clearly from this figure that there is a shift at the resonance peak

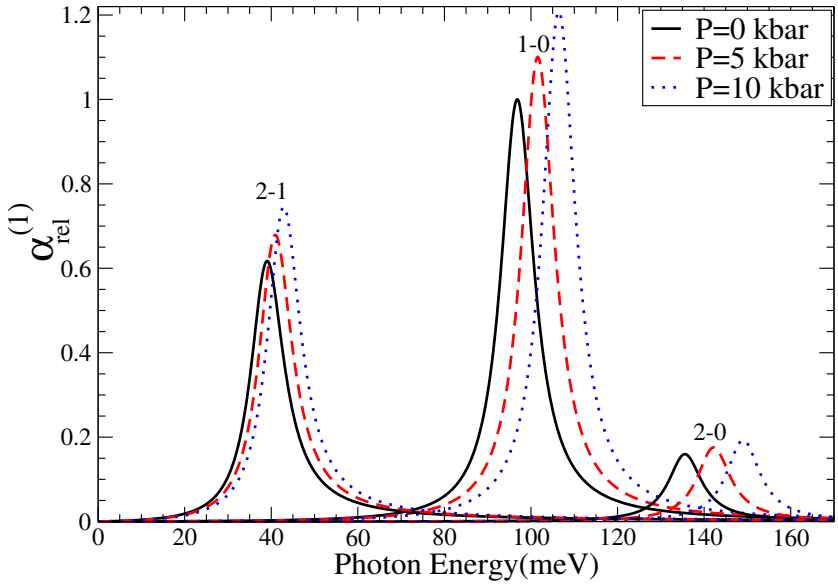

Fig. 2. The relative linear absorption coefficient of the (1-0), (2-1), (2-0) intersubband transitions and different applied hydrostatic pressure (solid-black) $P = 0$ kbar, (dashed-red) $P = 5$ kbar and (dotted-blue) $P = 10$ kbar. The values of the contact voltage and impurity density are: $V_c = 650$ meV and $N_{2d} = 7.5 \times 10^{12}\text{cm}^{-2}$.

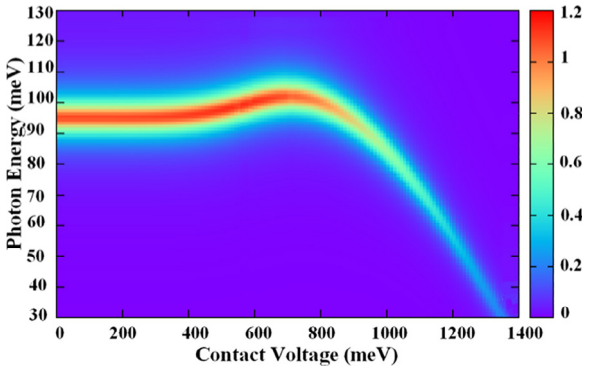

Fig. 3. Relative linear absorption coefficient of (1-0) intersubband transition as a function of the photon energy and contact voltage, with $N_{2d} = 7.5 \times 10^{12}\text{cm}^{-2}$ and $P = 5$ kbar.

positions with the hydrostatic pressure. The main reason for this resonance shift is the variation between energy intervals of two different electronic states $E_j - E_i$. Our results are compatible with others found in alike quantum structures [11,14,22,31]. Additionally, we show that the δ-FET allows an asymmetric potential configuration, so transitions (2-0) in this device are not forbidden.

Fig. 3 shows the linear absorption peak of the dominant intersubband transitions (1-0) as a function of the photon energy and contact voltage. We can see that when the contact potential increases, the amplitude of the linear absorption peak decreases. Furthermore, when the contact potential is greater than 700 meV, the linear absorption peak shifts to lower energies. This shift is due to a decrease of the energy difference between ground and first state as the contact potential increases.

The analytical expression of linear absorption peak as a function of photon energy and contact voltage is:

$$\left(h\omega', V_c'\right) = \boldsymbol{arg}\left[\boldsymbol{max}\beta^{(1)}\left(h\omega', V_c'\right)\right], \tag{11}$$

$$h\omega' = 95 - 4 \times 10^{-2}V_c' + 1.6 \times 10^{-4}V_c'^2 - 1.7 \times 10^{-7}V_c'^3. \tag{12}$$

In Figs. 4–7 we show our results for the confining potential profile, subband energies and wavefunctions, energy difference between ground and first excited state, relative linear and nonlinear absorption coefficient as well as the total relative absorption coefficient. In all these cases, we have fixed the impurity density at $3.5 \times 10^{12}\text{cm}^{-2}$.

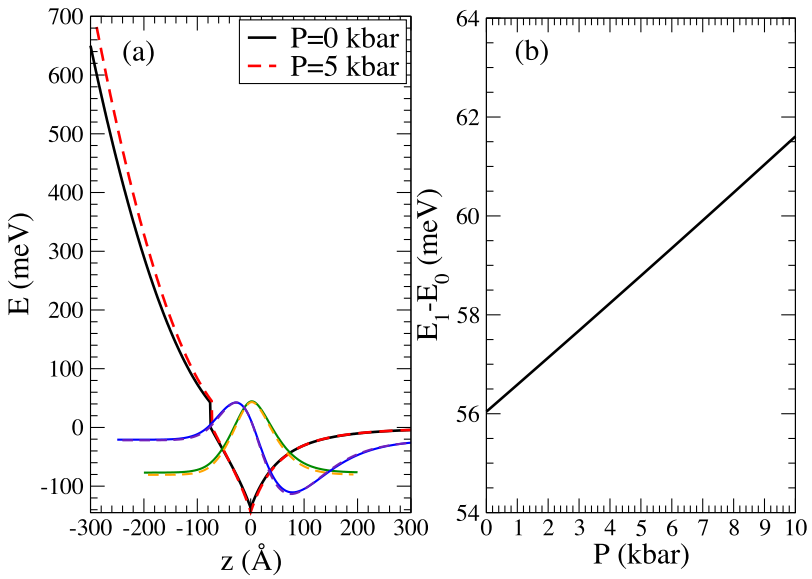

Fig. 4. (a) Confining potential profile, subband energies and the wave functions for P = 0 kbar (solid curves) and P = 5 kbar (dashed curves), with $V_c = 650$ meV and $N_{2d} = 3.5 \times 10^{12}\text{cm}^{-2}$. (b) Energy difference between the first excited state and ground state as a function of hydrostatic pressure, for $V_c = 650$ meV and $N_{2d} = 3.5 \times 10^{12}\text{cm}^{-2}$.

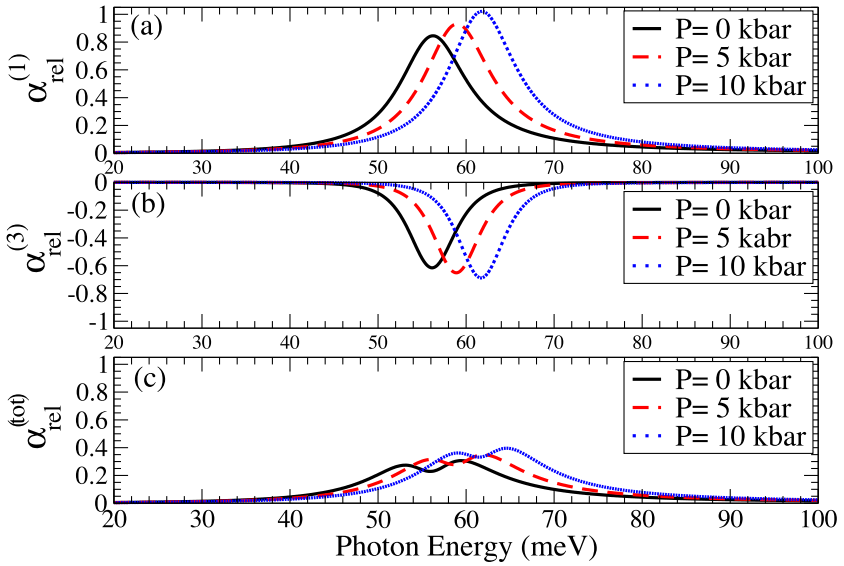

Fig. 5. Variation of the (a) relative linear absorption, (b) relative nonlinear absorption and (c) relative total intersubband absorption coefficient as a function of the photon energy for (solid-black) $P = 0$ kbar, (dashed-red) $P = 5$ kbar and (dotted-blue) P = 10 kbar. In this case only one resonant peak show up and corresponds to the (1-0) intersubband transition. The values of the contact voltage, impurity density and incident optical intensities are: $V_c = 650$ meV and $N_{2d} = 3.5 \times 10^{12}\text{cm}^{-2}$ and I = 0.1 MW/cm^2.

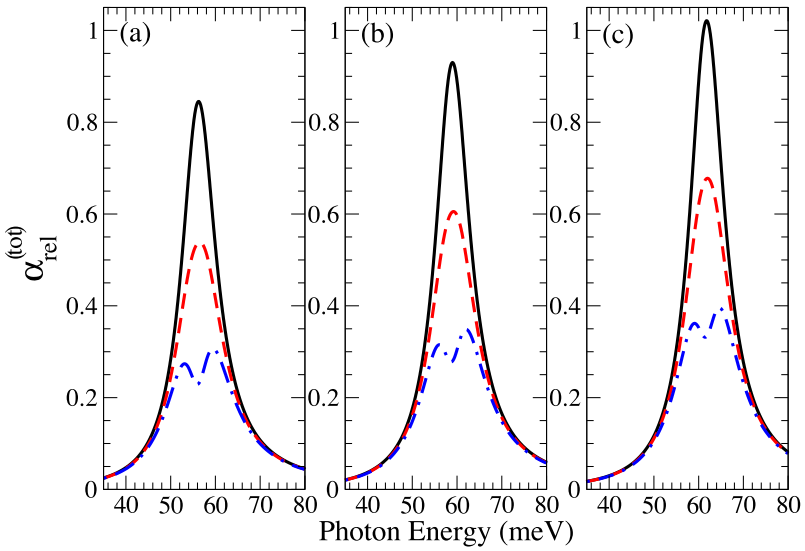

Fig. 6. Relative total intersubband absorption coefficient versus the photon energy for different optical intensities $I = 0,\ 0.05,\ 0.1$ MW/cm^2, from top to bottom, with $V_c = 650$ meV and $N_{2d} = 3.5 \times 10^{12}\text{cm}^{-2}$. (a) $P = 0$ kbar, (b) $P = 5$ kbar, (c) $P = 10$ kbar.

So, hereafter we will not refer to this quantity explicitly. Fig. 4(a) displays the change of the potential profile with respect to the applied hydrostatic pressure. We can see an asymmetric potential profile, which is very important for nonlinear optical applications. In Fig. 4(b) we have plotted the energy difference $E_1 - E_0$ as a function of the hydrostatic pressure for $V_c = 650$ meV. This result shows a blue shift in the optical properties of the system.

Fig. 5 shows the relative (a) linear, (b) nonlinear and (c) total absorption coefficient as a function of photon energy for three different pressure values 0, 5 and 10 kbar, with $N_{2d} = 3.5 \times 10^{12}\text{cm}^{-2}$, $V_c = 650$ meV and $I = 0.1$ MW/cm^2. Particularly, the linear absorption coefficient of (1-0) intersubband transition increases as the pressure increases as well. These results are similar to those shown in Fig. 3, the relative linear absorption coefficient increases and shifts towards higher energies. The blue shift of the resonant peak due to the pressure change can give valuable information about the variation of two energy levels in δ-FETs. Fig. 5(b) clearly shows that the nonlinear absorption coefficient reduces as the pressure increases. Besides, the resonance peak position shifts towards higher energies by increasing the pressure. In Fig. 5(c) we can see that the total

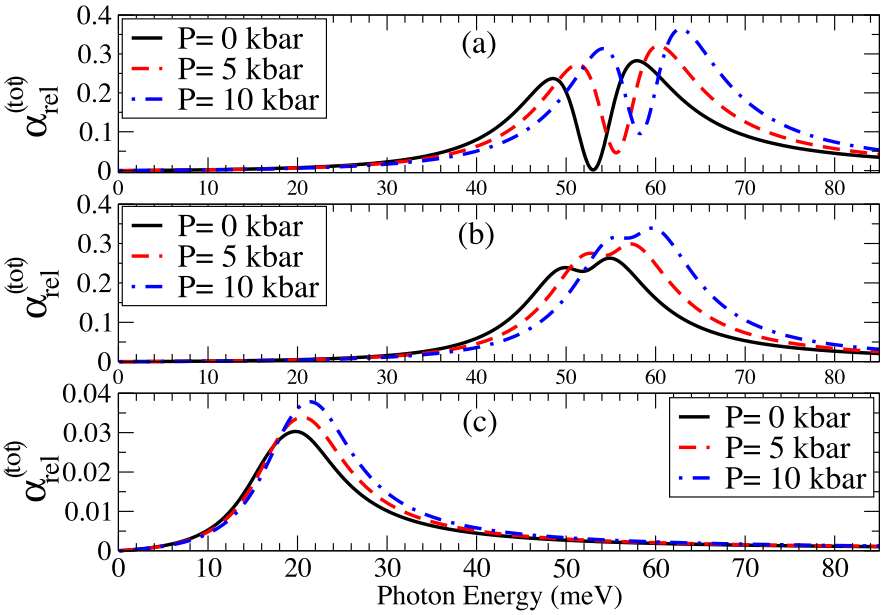

Fig. 7. The relative total optical absorption coefficient in a GaAs n-type delta doped field effect transistor as function of the incident photo energy for different hydrostatic pressure values $P = 0$, 5, 10 kbar for contact voltages: (a) $V_c = 400$ meV, (b) $V_c = 800$ meV and (c) $V_c = 1200$ meV. The optical intensity is and $I = 0.1$ MW/cm^2 and bidimensional density is $N_{2d} = 3.5 \times 10^{12}$cm^{-2}.

absorption coefficient has a similar behavior to the linear absorption coefficient. Because the linear and nonlinear absorption coefficients have opposite sign, the relative total absorption coefficient shifts to higher energies and the peak enhances as well. This shift is due to the increment in the energy difference between the first excited and the ground states as the hydrostatic pressure increases. A similar result is found in quantum wires [22,32].

In Fig. 6, we show the variations of the total absorption coefficient as a function of the photon energy for different pressures and optical intensities. As the incident optical intensity increases, for different values of pressure $P = 0$, 5, 10 kbar, the total absorption coefficient reduces. We want to highlight that the nonlinear term is related to the optical intensity as well as the linear term does not change with it. Likewise, we can see that there is no shift of the resonant peak at a constant pressure.

In Fig. 7 we show the total absorption coefficient for different hydrostatic pressure values $P = 0$, 5, 10 kbar for contact voltages (a) $V_c = 400$ meV, (b) $V_c = 800$ meV and (c) $V_c = 1200$ meV. When the contact voltage increases, the total absorption coefficients shift towards lower energies. The main reason for this behavior is the decrease in energy difference of two different electronic states, the ground state and first excited state. We can also see an increase of the total absorption coefficients as the contact voltage gets larger and a diminishing behavior of the no linear term as well. This means that contact voltage plays an important role in the intersubband absorption coefficient in δ-FET.

4. Conclusion

In summary, the effects of contact voltage and hydrostatic pressure on the subband structure and optical transitions in GaAs *n*-type δ-FET have been investigated. These external effects can be incorporated directly through their relation with the main input parameters of the systems in a simple and useful theoretical model at low pressure. In the case of the hydrostatic pressure through the pressure dependence of the electron effective mass and the dielectric constant. Our results indicate that hydrostatic pressure can induce an energy separation between intersubband energies, wavefunction confinement and height of the Schottky barrier. Absorption peaks change in magnitude and the absorption spectrum blue-shifts as hydrostatic pressure increases. Besides, the peak amplitude decreases and the spectrum red-shifts as the contact potential increases. Our results could be important for infrared optical device applications and useful in the design of devices based on hydrostatic pressure-dependent optical processes.

Acknowledgements

This work was partially supported by grants No. 252677 from *Conacyt* and *PAPIIT-IN104616* from UNAM México.

References

[1] I. Saidi, L. Bouzaïene, H. Mejri, H. Maaref, Mat. Sci. Eng. C 28 (2008) 831.
[2] E. Feddi, A. Talbi, M.E. Mora-Ramos, M. El Haouari, F. Dujardin, C.A. Duque, Phys. B 524 (2017) 64.
[3] O. Oubram, I. Rodríguez-Vargas, L.M. Gaggero-Sager, L. Cisneros- Villalobos, A. Bassam, J.G. Velásquez-Aguilar, M. Limón-Mendoza, Superlattice. Microst 100 (2016) 867.
[4] J.C. Martínez-Orozco, M.E. Mora-Ramos, C.A. Duque, J. Lumin 132 (2012) 449.
[5] J.C. Martínez-Orozco, M.E. Mora-Ramos, C.A. Duque, Phys. Status Solidi B 249 (2012) 146.
[6] A.V. Muravjov, D.B. Veksler, V.V. Popov, O.V. Polischuk, N. Pala, X. Hu, R. Gaska, H. Saxena, R.E. Peale, M.S. Shur, App. Phys. Lett. 96 (2010), 042105.
[7] D. Hofstetter, L. Diehl, J. Faist, W.J. Schaff, J. Hwang, L.F. Eastman, C.h. Zellweger, Appl. Phys. Lett. 80 (2002) 2991.
[8] R. Khordad, H. Bahramiyan, Phys. E 66 (2015) 107.
[9] E. Kasapoglu, F. Ungan, H. Sari, I. Sökmen, Phys. E 42 (2010) 1623.
[10] N. Raigoza, A.L. Morales, C.A. Duque, Braz. J. Phys. 36 (2006) 350.
[11] S. Liang, W. Xie, Phys. B 406 (2011) 2224.
[12] M.E. Mora-Ramos, L.M. Gaggero-Sager, C.A. Duque, Phys. E 44 (2012) 1335.
[13] J.C. Martínez-Orozco, K.A. Rodríguez-Magdaleno, J. Suarez-López, C.A. Duque, R.L. Restrepo, Superlattice. Microst 92 (2016) 166.
[14] O. Oubram, O. Navarro, L.M. Gaggero-Sager, J.C. Martínez-Orozco, I. Rodríguez-Vargas, Solid State Sci. 14 (2012) 440.
[15] E. Kasapoglu, U. Yesilgul, F. Ungan, I. Sökmen, H. Sari, Opt. Mate 64 (2017) 82.
[16] O. Oubram, L.M. Gaggero-Sager, A. Bassam, G.A. Luna-Acosta, PIER 110 (2010) 59.
[17] O. Oubram, L.M. Gaggero-Sager, O. Navarro, M. Ouadou, PIER 118 (2011) 37.
[18] J.C. Martínez-Orozco, I. Rodríguez-Vargas, C.A. Duque, M.E. Mora-Ramos, L.M. Gaggero-Sager, Phys. Status Solidi B 246 (2009) 581.
[19] I. Rodríguez-Vargas, M.E. Mora-Ramos, C.A. Duque, Microelectron. J. 39 (2008) 438.
[20] I. Karabulut, M.E. Mora-Ramos, C.A. Duque, J. Lumin. 131 (2011) 1502.
[21] M. Bajda, B. Piechal, F. Dybaa, A. Bercha, W. Trzeciakowski, J.A. Majewski, Phys. Status Solidi B 249 (2012) 217.
[22] R. Khordad, S. Kheiryzadeh Khaneghah, M. Masoumi, Superlattice. Microst 47 (2010) 538.
[23] G. Galindez-Ramirez, S.T. Pérez-Merchancano, H.P. Gutiérrez, J.D. Gonzalez, J. Phys. Conf. Ser. 245 (2010), 012012.
[24] L.M. Gaggero-Sager, R. Pérez-Álvarez, J. Appl. Phys. 78 (1995) 4566.
[25] L. Ioriatti, Phys. Rev. B 41 (1990) 8340.
[26] O. Oubram, M.E. Mora-Ramos, L.M. Gaggero-Sager, Eur. Phys. J. B 71 (2009) 233.
[27] D. Ahn, S.L. Chuang, IEEE J. Quantum Elect. 23 (1987) 2196.
[28] S. Sonmezoalu, F. Bayansal, G. Cankaya, Phys. B 405 (2010) 287.
[29] O. Oubram, L.M. Gaggero-Sager, I. Rodríguez-Vargas, Rev. Mex. Fis. 61 (2015) 281.
[31] U. Yesilgul, S. Sakiroglu, E. Kasapoglu, H. Sari, I. Sökmen, Superlattice. Microst 48 (2010) 106.
[32] M. Santhi, A.J. Peter, C.K. Yoo, Superlattice. Microst 52 (2012) 234.